ARCHIVES OF ACOUSTICS
12, 2, 113–128 (1987)

THE REFLECTION OF A GAUSSIAN PULSE OF A PLANE ULTRASONIC WAVE FROM RIGID AND ELASTIC SPHERES IN WATER

LESZEK FILIPCZYŃSKI, TAMARA KUJAWSKA

Department of Ultrasonics, IFTR, Polish Academy of Sciences
(00-049 Warszawa, ul. Świętokrzyska 21)

The authors have determined shapes and amplitudes of Gaussian pulses with limit frequencies equal to 2, 3, 10 and 20 kHz, which were reflected backwards from rigid and steel spheres with a 0.5 m radius, immersed in water. For this purpose spectral analysis, transmittance theorem and inverse Fourier transform were used. Reflected pulses exhibited two maxima corresponding to a specular reflection from the face surface of the sphere and to a creeping travelling wave around the sphere. These maxima were masked by many resonances inside of the elastic sphere. The masking effect decreases with the decrease of the limit frequency of the Gaussian pulse incident upon the sphere. In such a case the shape of the reflected pulse tends to a time derivative of the incident pulse. The peak to peak pressure of the reflected pulse remains unchanged in the range of limit frequencies under investigation. The measurement of the time interval between the first and second maximum of the reflected pulse makes it possible to determine the radius of the elastic sphere, if the limit frequency is sufficiently low.

Notation

A_m – auxiliary function
a – sphere radius
B_m – auxiliary function
c – wave velocity in water
c' – velocity of creeping wave
c_1 – velocity of longitudinal wave in the sphere
c_2 – velocity of transverse wave in the sphere
c_m – expansion coefficient
D_m – auxiliary function
E_m – auxiliary function
F_m – auxiliary function
f_g – limit frequency
f_∞ – shape function of the sphere
$h^{(2)} = j_m - jn_m$ – spherical Hankel function of the second type
$h_m^{(2)'}$ – derivation of function $h_m^{(2)}$ with respect to the argument
$j = \sqrt{-1}$

j_m – spherical Bessel function
j'_m – derivative of function j_m with respect to the argument
G_i – spectrum of the incident wave pulse
$k = \omega/c$ – wave number
m – natural number
n_m – spherical Neumann function
n'_m – derivative of function n_m with respect to the argument
P_m – Legendre polynomial
p_i – acoustic pressure of the incident wave
p_0 – acoustic pressure amplitude of the incident wave
p_s – acoustic pressure of scattered wave
q – constant
r – radial coordinate
s – constant
t – time
$x = \omega a/c$
$x_1 = \omega a/c_1$
$x_2 = \omega a/c_2$
β – constant
η_m – auxiliary quantity
θ – azimuth
$\lambda_g = c/f_g$ – limit wave length
ξ – auxiliary variable
ϱ – water density
ϱ_s – density of the sphere
τ – normalized time
ω – angular frequency
ω_g – limit angular frequency

1. Introduction

The reflection of ultrasonic waves from spherical objects immersed in water is of fundamental significance to many problems of ultrasound technology, such as hydroacoustic surveying. This problem has been undertaken in many papers. The first one to solve this problem theoretically for elastic spheres and a continuous wave was FARAN [4]. Later, other authors have pointed out a small mistake in FARAN'S very complex formulae [3, 12, 16]. Experimental research in the domain of the reflection effect, performed with the application of aluminium and brass spheres immersed in water in the range of $ka = 4.1 \div 57$, has confirmed the theory [8].

This paper deals with the effect of backward reflection of a Gaussian pulse of an ultrasonic wave incident upon rigid and elastic spheres immersed in water. It was accepted that a plane wave pulse, which is a time function near to a Dirac pulse, assumes a shape close to a Gauss pulse, due to imperfect generation and propagation conditions in water. Such a pulse incident upon a fixed sphere, is reflected from it and returns in the direction from which it was emited.

This paper is aimed at the determination of the shape and amplitude of the reflected pulse. It also tries to answer the question: Can any information concerning

the reflecting sphere be obtained on this basis? HASEGAWA'S formulae [9, 10, 11] describing the reflection of a continuous plane wave from an elastic sphere, with the correction made by ANSON and others [1], have been applied in this paper.

The procedure introduced by RUDGERS [18] and HICKLING [12] will be applied in order to analyse the reflection of pulses.

2. Gaussian pulse of an ultrasonic wave

A system of polar coordinates is being accepted (Fig. 1A). Considering axial symmetry we have two coordinates: r and θ. A Gaussian pulse of a plane wave moving along the z-axis ($z = r\cos\theta$) is the following time function (at a fixed value of z)

$$p_i = p_0 \exp(-\beta^2 t^2). \tag{1}$$

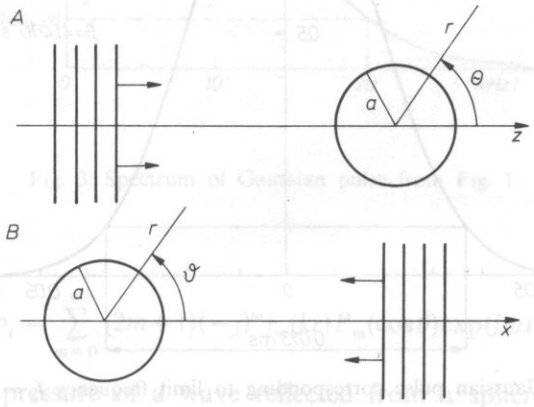

Fig. 1. A – Applied coordinate system – a plane progressive wave is incident upon sphere with radius a along the z-axis. This system was applied by authors of papers [4, 5, 11, 18]. B – Coordinate system applied by RSHEVKIN ([17], p. 258)

Assuming $p_0 = 1$ and applying a Fourier transform [13], we achieve the pulse spectrum in the following form

$$G_i(\omega) = \int_{-\infty}^{+\infty} p_i(t)\exp(-j\omega t)dt = \frac{\sqrt{\pi}}{\beta}\exp(-\omega^2/4\beta^2), \tag{2}$$

where the identity [6]

$$\int_{-\infty}^{+\infty} \exp(-u^2 s^2 \pm qs)ds = \frac{\sqrt{\pi}}{u}\exp(q^2/4u^2) \quad \text{for } u > 0, \tag{3}$$

was applied.

If we define the limit frequency f_g (as well as the limit angular frequency ω_g), as a frequency at which the spectrum amplitude is equal to 1/10 of the maximum value, then we have

$$\beta = \pi f_g / \sqrt{|\ln 0.1|} = 2.07 f_g = 0.329 \omega_g. \tag{4}$$

The shape of the Gaussian pulse which corresponds to the limit frequency $f_g = 20$ kHz is presented in Fig. 2, while its spectrum is shown in Fig. 3.

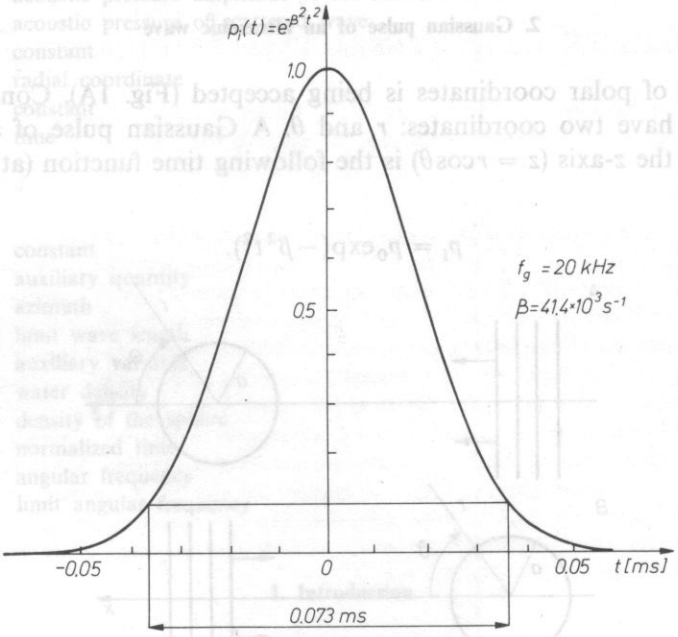

Fig. 2. Gaussian pulse corresponding to limit frequency $f_g = 20$ kHz

In further analysis we will introduce a dimensionless quantity $ka = \omega a/c$ in place of the angular frequency ω. Hence, we achieve the following expression, if we include factor a/c in the exponent in expression (2) and also include (4)

$$G_i(ka) = \frac{\sqrt{\pi}}{0.329\,\omega_g} \exp\left[-(ka)^2 / 0.433 \left(\frac{\omega_g a}{c} \right)^2 \right]. \tag{5}$$

3. Reflection of a continuous wave and a Gaussian pulse from rigid spheres

First of all we will determine the value of a continuous wave reflected from a rigid sphere. The acoustic pressure of a harmonic plane wave propagating in the direction $z = r\cos\theta$ (Fig. 1) has the following form [11, 9, 10]

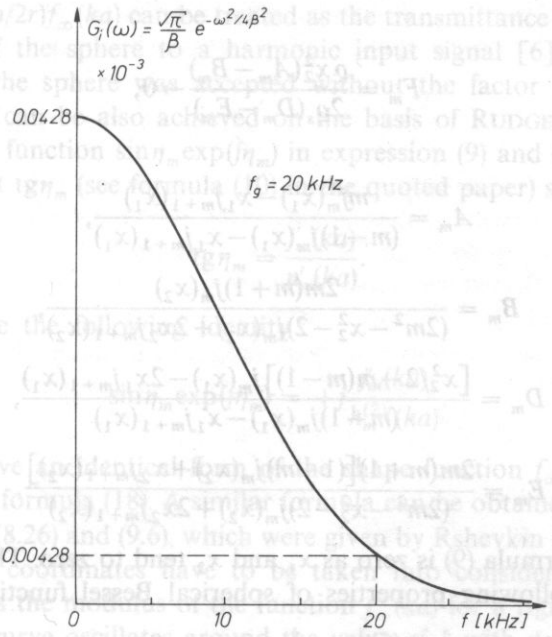

Fig. 3. Spectrum of Gaussian pulse from Fig. 1

$$p_i = \sum_{m=0}^{\infty} (2m+1)(-j)^m j_m(kr) P_m(\cos\theta)\exp(j\omega t) \tag{6}$$

while the acoustic pressure of a wave reflected from a sphere is expressed as

$$p_s = \sum_{m=0}^{\infty} (2m+1)(-j)^m c_m h_m^{(2)}(kr) P_m(\cos\theta)\exp(j\omega t). \tag{7}$$

Coefficient c_m is determined from boundary conditions on the surface of the sphere. In the case of an elastic sphere this coefficient is a function of: velocity of a longitudinal and transverse waves in the sphere, sphere density, wave velocity in the fluid surrounding the sphere, fluid density, frequency and radius of the sphere. This relationship becomes simpler in the case of a rigid sphere, because the velocity of longitudinal and transverse waves tends to infinity. Hence,

$$(c_1 \to \infty,\ c_2 \to \infty) \Rightarrow x_1 \to 0 \quad \text{and} \quad x_2 \to 0, \tag{7a, b}$$

and HASEGAWA'S formulae [8, 11, 1] for an elastic sphere can be simplified to the form for a rigid sphere, because then

$$c_m = \left[x j_m(x) - F_m j_m(x)\right] / \left[F_m h_m^{(2)}(x) - x h_m^{(2)\prime}(x)\right] \to -j_m'(x)/h_m^{(2)\prime}(x) \tag{8}$$

as

$$F_m = \frac{\varrho x_2^2 (A_m - B_m)}{2\varrho_s (D_m - E_m)} \to 0, \tag{9}$$

where

$$A_m = \frac{m j_m(x_1) - x_1 j_{m+1}(x_1)}{(m-1) j_m(x_1) - x_1 j_{m+1}(x_1)}, \tag{10}$$

$$B_m = \frac{2m(m+1) j_m(x_2)}{(2m^2 - x_2^2 - 2) j_m(x_2) + 2x_2 j_{m+1}(x_2)}, \tag{11}$$

$$D_m = \frac{[x_2^2/2 - m(m-1)] j_m(x_1) - 2x_1 j_{m+1}(x_1)}{(m-1) j_m(x_1) - x_1 j_{m+1}(x_1)}, \tag{12}$$

$$E_m = \frac{2m(m+1)[(1-m) j_m(x_2) + x_2 j_{m+1}(x_2)]}{(2m^2 - x_2^2 - 2) j_m(x_2) + 2x_2 j_{m+1}(x_2)}. \tag{13}$$

The limit of formula (9) is zero as x_1 and x_2 tend to zero. This could be shown by applying the following properties of spherical Bessel functions [15]

$$\frac{j_{m+1}(\xi)}{j_m(\xi)} \to \frac{\xi}{2m+3} \quad \text{for } \xi \to 0 \tag{14}$$

and the de l'Hospitals principle twice with respect to (9). Approximating the Hankel function by an asymptotic expression ([17], p. 211) for a distance much greater than the radius of the sphere, $r \gg a$

$$h_m^2(kr) = \frac{1}{kr} \exp\left[-j\left(kr - \frac{m+1}{2}\pi\right)\right] \tag{15}$$

including identity

$$(-j)^m \exp[j(m+1)\pi/2] = +j, \tag{16}$$

and assuming backward reflection ($\theta = 180°$)

$$P_m(\cos\theta) = (-1)^m \tag{17}$$

we achieve from formulae (7) and (8) the final form of the formula for the acoustic pressure of a continuous wave reflected from a rigid sphere [5]

$$p_s = \frac{a}{2r}\left[\frac{-2}{ka} \sum_{m=0}^{\infty} j(2m+1)(-1)^m \frac{j_m'(ka)}{h_m^{(2)'}(ka)}\right] \exp[-j(kr - \omega t)]$$

$$= \frac{a}{2r} f_\infty(ka) \exp[-j(kr - \omega t)]. \tag{18}$$

The expression in first square brackets in formula (18) is called the shape function of the backward reflection from a sphere in the far field. It is denoted by

$f_\infty(ka)$. Function $(a/2r)f_\infty(ka)$ can be treated as the transmittance of the sphere which is the response of the sphere to a harmonic input signal [6]. In paper [6] the transmittance of the sphere was accepted without the factor $a/2r$.

Formula (18) can be also achieved on the basis of RUDGERS paper [18]. The author introduced function $\sin\eta_m \exp(j\eta_m)$ in expression (9) and (11) in his paper. It can be proved that $\operatorname{tg}\eta_m$ (see formula (10) in the quoted paper) satisfies relationship

$$\operatorname{tg}\eta_m = \frac{j'_m(ka)}{n'_m(ka)}. \tag{19}$$

Then we have the following identity

$$\sin\eta_m \exp(j\eta_m) = +j\frac{j'_m(ka)}{h_m^{(2)\prime}(ka)}. \tag{20}$$

Hence, we have an identical form of the shape function $f_\infty(ka)$ as in the first square brackets in formula (18). A similar formula can be obtained also on the basis of formulae (8.24), (8.26) and (9.6), which were given by Rshevkin [17]. In such a case differently defined coordinates have to be taken into consideration (Fig. 1B).

Fig. 4 presents the modulus of the function $f_\infty(ka)$ for a rigid sphere (curve R). For $ka > 10$ this curve oscillates around the value of 1 with decaying oscillations.

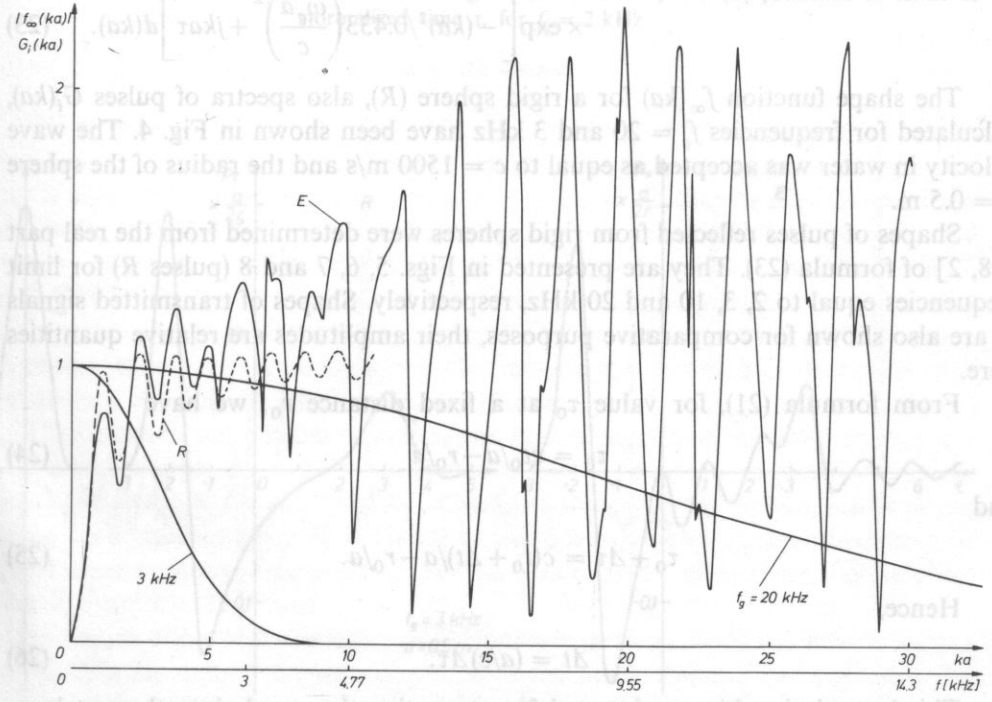

Fig. 4. Shape function $f_\infty(ka)$ for a rigid (R) and steel (E) sphere, and spectra of a Gaussian pulse with limit frequency $f_g = 20$ kHz and 3 kHz (related to the maximal value). Sphere radius $a = 0.5$ m

When the wave incident upon the sphere has the shape of a pulse, then two variables, r and t, are substituted by one dimensionless variable in the following form [18]

$$\tau = (ct - r)/a. \tag{21}$$

This procedure is justifiable, because the same shape of a pulse is obtained at a fixed time t when its shape is observed in terms of distance r, or on the contrary at a fixed distance r when its shape is observed in time t.

The pulse of a reflected wave will be presented in the domain of time normalized by expression (21) with the application of the linear theory of networks [14]. To this end an inverse Fourier transform was determined from the product of the transmittance of the sphere, $a/2rf_\infty(ka)$, and pulse spectrum $G_i(ka)$. Including formulae (18) and (5) we have

$$p_s(\tau) = \frac{1}{2\pi}\int_{-\infty}^{+\infty} \frac{a}{2r} f_\infty(ka) G_i(ka) \exp(jka\tau) d(ka) \tag{22}$$

or in full notation

$$p_s(\tau) = \frac{a}{4\pi r}\int_{-\infty}^{+\infty} \left[\frac{-2}{ka}\sum_{m=0}^{\infty} j(2m+1)(-1)^m \frac{j'_m(ka)}{h_m^{(2)\nu}(ka)}\right] \frac{\sqrt{\pi}}{0.329\omega_g} \times$$

$$\times \exp\left[-(ka)^2/0.433\left(\frac{\omega_g a}{c}\right)^2 + jka\tau\right] d(ka). \tag{23}$$

The shape function $f_\infty(ka)$ for a rigid sphere (R), also spectra of pulses $G_i(ka)$, calculated for frequencies $f_g = 20$ and 3 kHz have been shown in Fig. 4. The wave velocity in water was accepted as equal to $c = 1500$ m/s and the radius of the sphere $a = 0.5$ m.

Shapes of pulses reflected from rigid spheres were determined from the real part [18, 2] of formula (23). They are presented in Figs. 5, 6, 7 and 8 (pulses R) for limit frequencies equal to 2, 3, 10 and 20 kHz, respectively. Shapes of transmitted signals T are also shown for comparative purposes, their amplitudes are relative quantities here.

From formula (21), for value τ_0 at a fixed distance r_0, we have

$$\tau_0 = ct_0/a - r_0/a \tag{24}$$

and

$$\tau_0 + \Delta\tau = c(t_0 + \Delta t)/a - r_0/a. \tag{25}$$

Hence,

$$\Delta t = (a/c)\Delta\tau. \tag{26}$$

This last relationship can be used for converting the τ-scale into the t-scale – different for every radius a of the sphere.

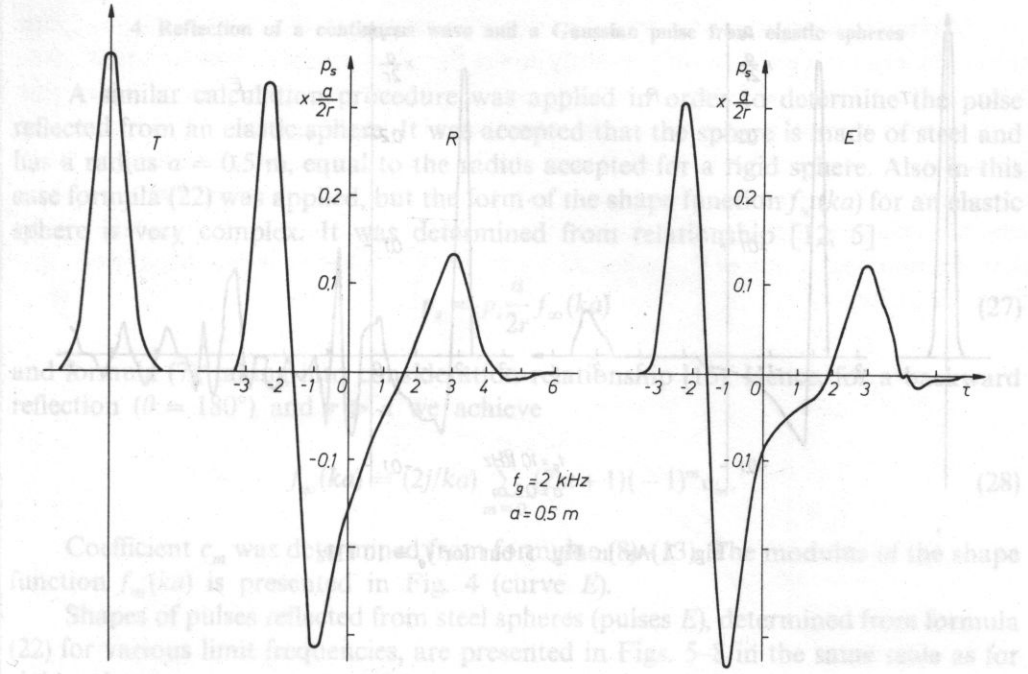

Fig. 5. Transmitted pulse (T), reflected from a rigid (R) and steel sphere (E) presented in terms of normalized time τ, for $f_g = 2$ kHz

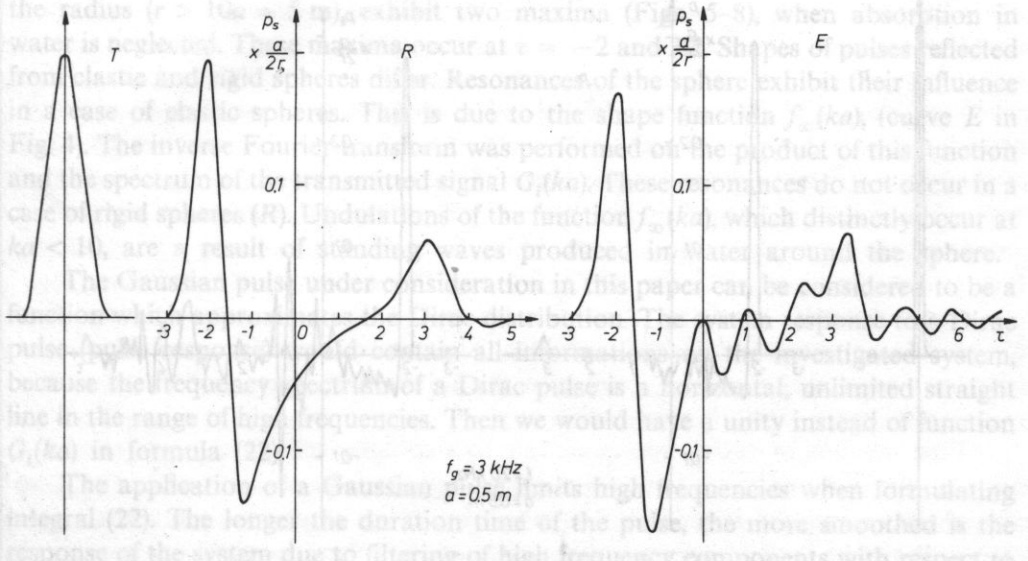

Fig. 6. As in Fig. 5 but for $f_g = 3$ kHz

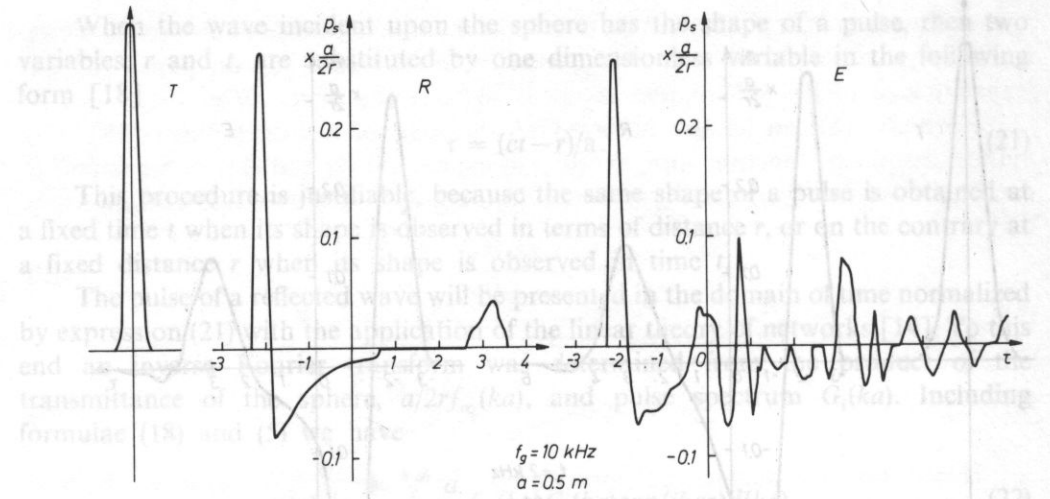

Fig. 7. As in Fig. 5 but for $f_g = 10$ kHz

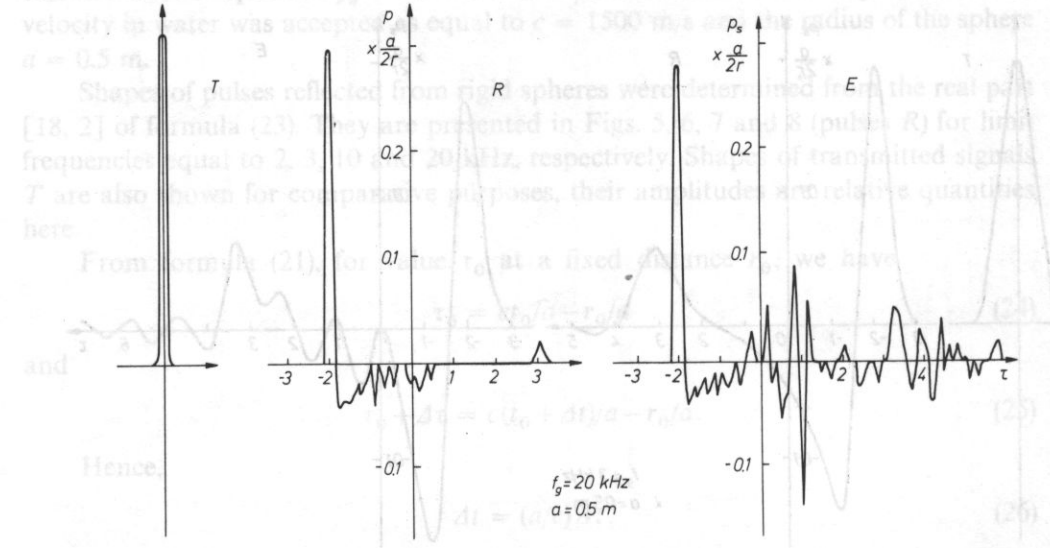

Fig. 8. As in Fig. 5 but for $f_g = 20$ kHz

4. Reflection of a continuous wave and a Gaussian pulse from elastic spheres

A similar calculation procedure was applied in order to determine the pulse reflected from an elastic sphere. It was accepted that the sphere is made of steel and has a radius $a = 0.5$ m, equal to the radius accepted for a rigid sphere. Also in this case formula (22) was applied, but the form of the shape function $f_\infty(ka)$ for an elastic sphere is very complex. It was determined from relationship [12, 5]

$$p_s = p_i \frac{a}{2r} f_\infty(ka) \tag{27}$$

and formula (7), taking into consideration relationship (15). Hence, for a backward reflection ($\theta = 180°$) and $r \gg a$ we achieve

$$f_\infty(ka) = (2j/ka) \sum_{m=0}^{\infty} (2m+1)(-1)^m c_m. \tag{28}$$

Coefficient c_m was determined from formulae (8)–(13). The modulus of the shape function $f_\infty(ka)$ is presented in Fig. 4 (curve E).

Shapes of pulses reflected from steel spheres (pulses E), determined from formula (22) for various limit frequencies, are presented in Figs. 5–8 in the same scale as for rigid spheres.

5. Results and discussion

Pulses reflected backwards from rigid spheres at a great distance with respect to the radius ($r > 10a = 5$ m), exhibit two maxima (Figs. 5–8), when absorption in water is neglected. These maxima occur at $\tau = -2$ and 3.2. Shapes of pulses reflected from elastic and rigid spheres differ. Resonances of the sphere exhibit their influence in a case of elastic spheres. This is due to the shape function $f_\infty(ka)$, (curve E in Fig. 4). The inverse Fourier transform was performed on the product of this function and the spectrum of the transmitted signal $G_i(ka)$. These resonances do not occur in a case of rigid spheres (R). Undulations of the function $f_\infty(ka)$, which distinctly occur at $ka < 10$, are a result of standing waves produced in water around the sphere.

The Gaussian pulse under consideration in this paper can be considered to be a function which approximates the Dirac distribution. The system response to a Dirac pulse (pulse response) would contain all informations on the investigated system, because the frequency spectrum of a Dirac pulse is a horizontal, unlimited straight line in the range of high frequencies. Then we would have a unity instead of function $G_i(ka)$ in formula (22).

The application of a Gaussian pulse limits high frequencies when formulating integral (22). The longer the duration time of the pulse, the more smoothed is the response of the system due to filtering of high frequency components with respect to the transmittance function of the sphere.

Maximal amplitudes of reflected pulses with respect to the limit frequency f_g are shown in Fig. 9. They are only slightly lower for steel spheres than for rigid ones. This is due to great differences between specific acoustic impedances of water and steel, so only a small part of the energy penetrates into steel spheres, while it does not penetrate into rigid spheres at all. These amplitudes decrease rapidly when the limit frequency f_g is decreased. However, if we take into consideration the overshoot, which is observed directly after the first maximum (for $-2 < \tau < 0$), then we observe that the maximal value of the reflected signal peak to peak is independent from the limit frequency.

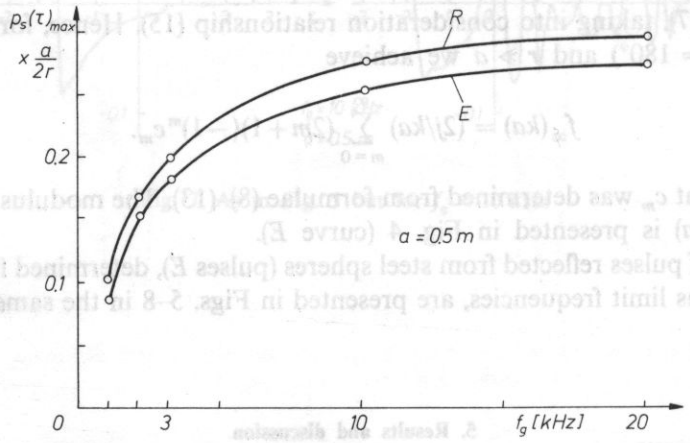

Fig. 9. Maximal amplitudes (positive) of a pulse reflected from rigid (R) and elastic (E) spheres in terms of limit frequency f_g (at $\tau = -2$)

Figs. 10 and 11 present transmitted pulses and first maxima of received pulses placed over them for $f_g = 20$ and 3 kHz. In the second case it is visible that the shape of the reflected pulse approaches the shape of the time derivative of the transmitted pulse. This can be explained by the shape of the transmittance curve $(a/2rf_\infty(ka)$ for small values of ka (at $a/2r = \text{const}$) (Fig. 4) similarly as for a differentiating four-terminal network RC, for which it would be a straight inclined line.

The differentiation of the reflected pulse can be also explained by the fact that for $ka < 1$ components of the waves incident upon the sphere with higher frequencies (shorter wave lengths) are reflected from the sphere with greater amplitudes than components with lower frequencies.

First maxima of pulses, corresponding to a specular reflection, occur always at $\tau = -2$, because the initial time $t = 0$ was accepted in the moment when the wave propagating along the z-axis (Fig. 1A) would reach the origin of coordinates, $r = 0$. Hence, the wave is incident upon the surface of the sphere in point $r = -a$ in the time $t = -a/c$. Substituting these in formula (21) we achieve $\tau = -2$.

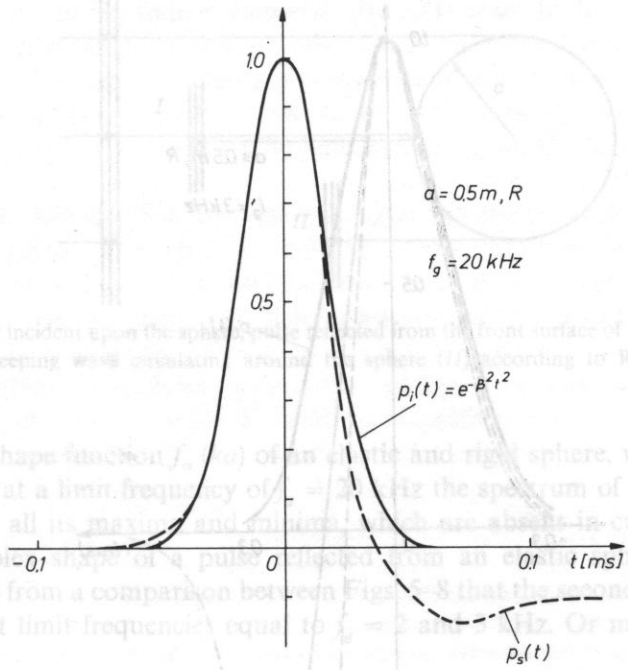

Fig. 10. Shape of transmitted pulse p_i with the first maximum of the pulse p_s reflected from a rigid sphere drawn over it, for f_g = 20 kHz

The second maximum of a reflected pulse was observed in all cases at $\tau = 3.2$. Its value is much lower than that of the first maximum. Because this effect also occurs with rigid spheres, it must be related to phenomena occuring outside the sphere. Such an effect had been observed by RUDGERS [18] in his theoretical paper. He related it to a creeping wave, which propagates around the sphere with a velocity only slightly lower than that in water. The path of a creeping wave, according to this author, is shown in Fig. 12. The first maximum is produced by a direct reflection of a pulse from the front surface of the sphere; the second one occurs much later, when the wave has propagated around the sphere. The difference of propagation time was equal to $\Delta\tau = 5.2$ in all cases. This corresponds to velocity

$$c' = \pi a/(\Delta\tau a/c - 2a/c) = 0.98c, \tag{29}$$

where the numerator denotes the path around the hemisphere travelled by the pulse of a creeping wave, and the denominator denotes the time of this process, calculated from relationship (26).

The idea of a wave travelling around the sphere seems justfiable by the fact that the curve $f_\infty(ka)$ exhibits an oscillatory behaviour for a rigid sphere. For, this testifies to the existence of waves around the sphere, which cause inteferences in the steady state (see curve R in Fig. 4).

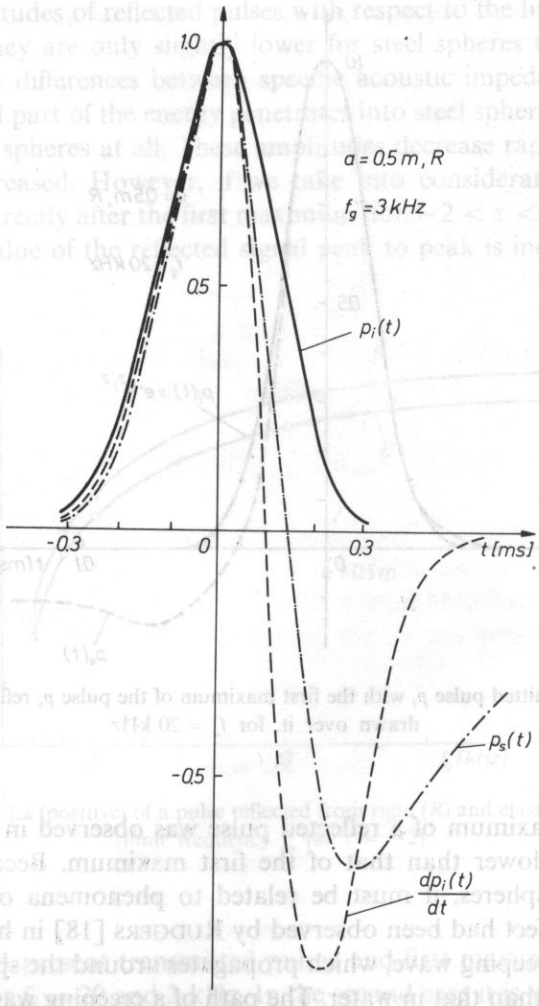

Fig. 11. Shape of transmitted pulse p_i with the derivative dp_i/dt and first maximum of the pulse p_s reflected from a rigid sphere drawn over it, for f_g = 3 kHz; in order to compare more easily these functions, they have been shifted in time and their maximal positive values have been equalized

Therefore, it is possible to determine the unknown radius of the sphere on the basis of the time interval $\Delta t_{\mathrm{I-II}}$ measurement, from formula

$$a = c' \Delta t_{\mathrm{I-II}} (\pi + 2c'/c)^{-1} \approx c \Delta t_{\mathrm{I-II}} (\pi + 2)^{-1}. \tag{30}$$

However, it may be difficult to determine the second maximum for a case of real (elastic) spheres. It can be seen from comparison between Figs. 5–8 that the shape of a pulse reflected from an elastic sphere becomes similar to a pulse reflected from a rigid sphere at lower limit frequencies. This effect can be explained on the basis of Fig. 4. The spectrum of a Gaussian pulse at a limit frequency of 3 kHz includes such

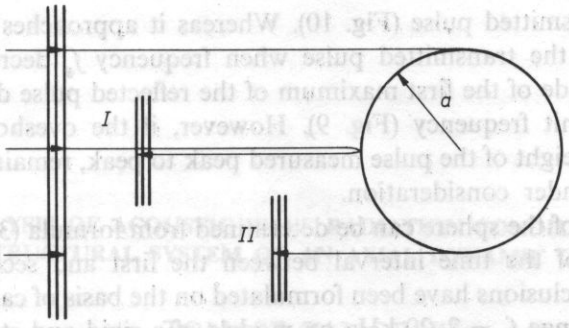

Fig. 12. Pulse (T) incident upon the sphere, pulse reflected from the front surface of the sphere (I) and pulse of a creeping wave circulating around the sphere (II) according to RUDGERS [18]

parts of the shape function $f_\infty(ka)$ of an elastic and rigid sphere, which have similar shape. While at a limit frequency of $f_g = 20$ kHz the spectrum of this pulse includes curve E with all its maxima and minima, which are absent in curve R. Hence, we have a complex shape of a pulse reflected from an elastic sphere (Fig. 8E).

It results from a comparison between Figs. 5–8 that the second maximum can be determined at limit frequencies equal to $f_g = 2$ and 3 kHz. Or more general in the case when

$$\lambda_g/a = 1\text{–}1.5. \tag{31}$$

Besides a creeping wave which circulates the sphere once, also cases of repeated circulation can take place, but amplitudes of these waves are two orders of magnitude smaller [18]. Therefore, they can be neglected.

6. Conclusions

a) A Gaussian pulse of a plane ultrasonic wave incident upon a sphere produces a reflected pulse, which exhibits two maxima for a rigid sphere model. The first maximum is formed due to a direct specular reflection of a wave from the front surface of a sphere (at $\tau = -2$, see curves R in Figs. 5–8), while the second one (at $\tau = 3.2$) is formed due to a creeping wave which circulates the sphere.

b) The second maximum in the case of an elastic sphere (steel) is masked by many maxima and minima, produced by internal resonances of the sphere (see curve E in Figs. 5–8).

c) The second maximum can be determined when relationship (31) is satisfied. The masking effect decays then.

d) The lower the limit frequency f_g the higher the value of the second maximum, equally for a rigid and elastic sphere. The second maximum becomes more easily detectable then.

e) At a limit frequency of $f_g = 20$ kHz, the shape of the first maximum is very

much like the transmitted pulse (Fig. 10). Whereas it approaches the shape of the time derivative of the transmitted pulse when frequency f_g decreases (Fig. 11).

f) The amplitude of the first maximum of the reflected pulse decreases with the decrease of the limit frequency (Fig. 9). However, if the oveshoot is taken into account, then the height of the pulse measured peak to peak, remains constant in the frequency range under consideration.

g) The radius of the sphere can be determined from formula (30) on the basis of the measurement of the time interval between the first and second maximum.

The above conclusions have been formulated on the basis of calculations carried out in frequency range $f_g = 2$–20 kHz on models of a rigid and steel sphere with a radius of $a = 0.5$ m. It was found that at low frequencies the incident Gaussian pulse does not "see" the interior of the sphere – is unresponsible to its internal structure. While at the same time the magnitude of the echo is independent from frequency, because of the overshoot in the reflected pulse.

References

[1] I. ANSON, R. CHIVERS, H. STOCKDALE, *The calculation of Y_p for suspended sphere radiometer targets*, Acustica, **48**, 304 (1981).

[2] D. CHAMPENEY, *Fourier transforms and their physical applications*, Academic Press, London, 14, 1973.

[3] L. DRAGONETTE, M. VOGT, L. FLAX, W. NEUBAUER, *Acoustic reflection from elastic spheres II. Transient analysis*, J. Acoust. Soc. Am., **23**, 4, 405–418 (1974).

[4] J. FARAN, *Sound scattering by solid cylinders and spheres*, J. Acoust. Soc. Am., **23**, 4, 405–418 (1951).

[5] L. FILIPCZYŃSKI, *Detectability of calsifications in breast tissues by the ultrasonic echo method*, Archives of Acoustics, **8**, 3, 209 (1983).

[6] C. GAZANHES, J. SESSAREGO, J. HERAULT, J. LEANDRE, *Fonctions de transfert et reponses impulsionnelles de shperes rigides et elastiques*, Acoustica, **52**, 5, 267 (1983).

[7] I. GRADSHTEIN, I. RISHIK, *Tablicy integralow, sum, rjadow i proizwedenii*, Nauka, Moskwa, 321, 1971.

[8] L. HAMPTON, C. MCKINEY, *Experimental study of the scattering of acoustic energy from solid metal spheres in water*, J. Acoust. Soc. Am., **33**, 5, 664–673 (1961).

[9] T. HASEGAWA, *Comparison of two solutions for acoustic pressure on a sphere*, J. Acoust. Soc. Am., **61**, 6, 1445–1448 (1971).

[10] T. HASEGAWA, Y. WATANABE, *Acoustic radiation pressure on an absorbing sphere*, J. Acoust. Soc. Am., **63**, 6, 1733–1737 (1978).

[11] T. HASEGAWA, K. YOSIOKA, *Acoustic radiation force on a solid elastic sphere*, J. Acoust. Soc. Am., **46**, 5 P2, 1139–1143 (1969).

[12] R. HICKLING, *Analysis of echoes from a solid elastic sphere in water*, J. Acoust. Soc. Am., **39** (1966).

[13] P. HWEI HSU, *Fourier analysis, Simon and Schuster*, New York, 74, 1970.

[14] Z. KLONOWICZ, Z. ZURZYCKI, *Theory of networks*, t. I, PWN, Warszawa 1983 (in Polish).

[15] P. MORSE, K. INGARD, *Theoretical acoustics*, McGraw-Hill, New York, 338, 1968.

[16] W. NEUBAUER, M. VOGT, L. DRAGONETTE, *Acoustic reflection from elastic spheres*, I. Steady-state signals, J. Acoust. Soc. Am., **55**, 1123–1129 (1974).

[17] C. RSHEVKIN, *Kurs lekcij po teorii zwuka*, Izd. Moskovskovo Universiteta, Moskwa 1960.

[18] A. RUDGERS, *Acoustical pulses scattered by a rigid sphere in a fluid*, J. Acoust. Soc. Am., **45**, 4, 900–910 (1969).

Received on June 12, 1986; revised version on January 15, 1987.